



EXPERIMENTAL STUDY ON EFFECTS OF HEIGHT OF LATERAL FORCES, COLUMN REINFORCEMENT AND WALL REINFORCEMENTS ON SEISMIC BEHAVIOR OF CONFINED MASONRY WALLS

Koji Yoshimura¹, Kikuchi Kikuchi¹, Masayuki Kuroki², Hideko Nonaka², Kyong Tae Kim³,
Reezang Wangdi³ and Ayasa Oshikata³

SUMMARY

In order to investigate the effect of the height of application point of lateral loads and reinforcing steel bars in walls and columns in improving the seismic behavior of confined concrete block masonry walls, an experimental research program is conducted. A total of twelve one-half scale specimens are tested under repeated lateral loads. Specimens are tested to failure with increasing maximum lateral drifts while a vertical axial load was applied and maintained constant. The specimens adopted are two-dimensional (2D) hollow concrete block masonry walls with different parameters such as shear span ratio, inflection point and percent of reinforcement in confining columns and walls. The heights of inflection point of walls considered are 0.67, 1.08 and 1.1 times the height of the wall measured from the top of foundation beam. The constant vertical axial stresses applied are 0, 0.84 and 1.08MPa, while the amount of reinforcements in horizontal and vertical directions are 0%, 0.08% and 0.18% and 0.18%, 0.36% and 0.64% respectively. Test results obtained for each specimen include cracking patterns, load-deflection data, and strains in reinforcement and walls in critical locations. Analysis of test data showed that above parameters generate a considerable effect on the seismic performance of confined concrete block masonry walls.

INTRODUCTION

The use of some type of reinforcement is expected to be the most effective in reducing the earthquake damage of masonry constructions made distinctively with different materials, which in this case, is confined concrete masonry walls. Confined concrete masonry consists of masonry panels, made of hollow concrete units or blocks, portland cement mortar, and reinforced concrete (R/C) beams and columns along lateral and top boundaries. The objectives of the confining R/C elements are to tie together the walls,

¹ Professor, Dr. Eng., Department of Architectural Engineering, Oita University, Oita, 870-1192, Japan.

² Research Associate, Department of Architectural Engineering, Oita University, Oita, 870-1192, Japan.

³ Graduate Student, Department of Architectural Engineering, Oita University, Oita, 870-1192, Japan.



Fig. 1 CM wall buildings under construction (Mexico, 1993)

floors and roofs, as well as to provide some out-of-plane flexural strength. In line with these objectives, confined masonry (CM) has been adopted in several developing countries, especially in Latin American countries of Mexico, Colombia, El Salvador, etc. as well as in east Asian countries such as in the People's Republic of China. Fig. 1 shows the pictures of some of the CM wall buildings under construction in Mexico. In some developing countries, small dwellings and single-family houses are mainly built of confined masonry, however, multi-family buildings, up to several stories high, are also constructed with this system. Although, the confined masonry wall system has been widely accepted into the low- and medium-rise masonry buildings as an effective seismic structural system, there were quite few examples in which a structural damage occurred during earthquakes mainly due to absence of wall reinforcements in horizontal and vertical directions.

To investigate the effect of vertical axial load, wall height to span ratio and wall reinforcements on the seismic performance of confined concrete masonry walls, the experimental research reported in this paper is conducted.

WALL SPECIMENS AND MATERIAL PROPERTIES

A total of twelve confined concrete hollow block masonry wall specimens were designed and constructed. Their details with different parameters such as aspect ratios, inflection points, amount of horizontal and vertical wall reinforcement, etc are listed in Table 1. Fig.2 shows one of the typical specimens. All the specimens are approximately one-half scale models of one-bay-one-story masonry walls using hollow concrete block masonry units (190mmx390mmx100mm) with Grade C in the Japanese Industrial Standards (JIS). The thickness of all the walls is 100mm and these were confined by cast-in-place R/C columns with 100mmx100mm cross-sections along their extreme edges and T-shaped R/C collar beams along their tops. These specimens were tested under the repeated lateral forces, and constant axial compression loads of 0, 0.48 and 0.84MPa respectively and these

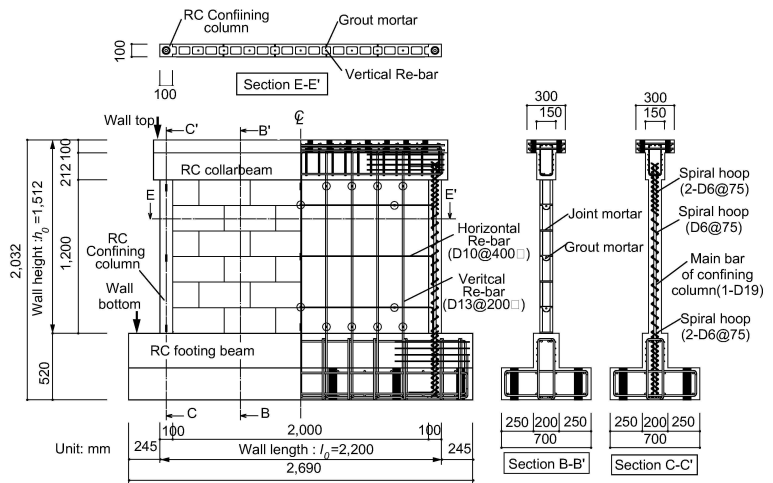


Fig. 2 Typical test specimen

specimens are classified into two test series, L-series and H-series, depending upon the height of applied repeated lateral forces. Each of the specimens is designated by the symbol code, such as 1.5L22-H0V0.36-0, 0.8L10-H0.18V0.18-LC, 0.7H19-H0V0.64-HC, etc. The first numeric symbols “1.5”, “0.8” and “0.7” represent the aspect ratios (or height to span ratios) respectively. The second letters “L” or “H” indicates the location of the point of application of lateral forces (or inflection point of the flexural deformation of the walls) is “Low” (taken as 0.67 times the wall height) or “High” (equal to 1.08 and 1.1 times the wall height) respectively, and the numerals “19”, “22” and “25” represent the size of longitudinal Re-bars provided in each of the confining R/C column sections such as D19 (or #6), D22 (or #7) and D25 (or #8) with circular spiral hoops of D6 (or #2) as shown in Fig.2. The symbol “H” followed by numerals 0, 0.08 and 0.18 indicate the percentage of horizontal reinforcement in wall and in the same manner the letter “V” with the numerals 0.18, 0.36 and 0.64 represent the percentage of vertical wall reinforcement. In the last symbol, “0” means the zero vertical axial stress or no vertical load was applied; “LC” and “HC” represent the axial stresses of 0.84MPa and 1.80MPa respectively corresponding to the low- and high-level of constant vertical loads, which are termed as Low Compression and High Compression in this paper. For the specimens from (1) to (4) given in Table 1, shear span ratio and ratio of tensile reinforcement of confining columns are taken as the parameters, while the later had been considered as parameter for the specimens from (5) to (8). The horizontal and vertical wall reinforcement ratios are taken as the test parameters for the remaining specimens from (9) to (12).

The compressive strengths and mechanical properties of the materials used for the specimens are shown in Tables 2 and 3, which are the average of at least three measurements.

Table 1 List of test specimens

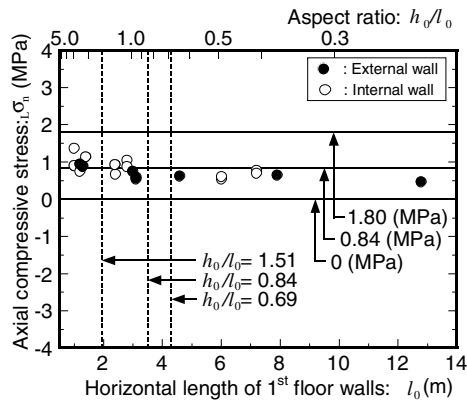
Specimen	Aspect ratio h_0/l_0	Inflection height ratio h'/h_0	Shear span ratio M/Qd $(=h'/d)$	Percent of tension steel $p_t = a_t / (t \cdot d)$ (%)	Percent of horizontal Re-bar p_h (%)	Percent of vertical Re-bar p_v (%)	Vertical axial stress σ_0 (MPa)
(1) 1.5L22-H0V0.36-0	1.51	0.67 (L)	1.07	0.41 (22)	0 (H0)	0.36 (D13 @200) (V0.36)	0 (0)
(2) 1.5H22-H0V0.36-0	(1.5)	1.11 (H)	1.77				
(3) 0.8L22-H0V0.36-0	0.84 (0.8)	0.67 (L)	0.58	0.22 (22)			
(4) 0.8H22-H0V0.36-0		1.11 (H)	0.96				
(5) 0.8L10-H0.18V0.18-LC		0.67 (L)	0.58	0.58	0.04 (10)	0.18 (H0.18)	0.18 (D10 @400) (V0.18)
(6) 0.8L16-H0.18V0.18-LC					0.11 (16)		
(7) 0.8L19-H0.18V0.18-LC	0.16 (19)						
(8) 0.8L25-H0.18V0.18-LC	0.29 (25)						
(9) 0.7H19-H0.08V0.64-LC	0.69 (0.7)	1.08 (H)	0.76	0.13 (19)	0.08 (H0.08)	0.64 (D13 @200) (V0.64)	0.84 (LC)
(10) 0.7H19-H0.18V0.64-LC					0.18 (H0.18)		
(11) 0.7H19-H0V0.64-LC					0 (H0)		
(12) 0.7H19-H0V0.64-HC							

Table 2 Mechanical properties of concrete, joint mortar and prism

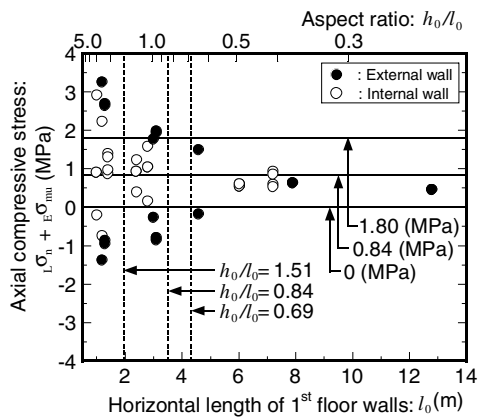
Specimen	Concrete		Joint mortar (MPa)	Prism (MPa)
	Column (MPa)	Beam (MPa)		
(1) 1.5L22-H0V0.36-0	30.8	30.2	38.0	19.9
(2) 1.5H22-H0V0.36-0	31.4	31.0	33.0	18.8
(3) 0.8L22-H0V0.36-0	27.6	28.9	36.5	17.3
(4) 0.8H22-H0V0.36-0	30.2	31.0	36.2	19.3
(5) 0.8L10-H0.18V0.18-LC	38.1	32.8	41.9	19.0
(6) 0.8L16-H0.18V0.18-LC	35.5	33.5	40.4	18.9
(7) 0.8L19-H0.18V0.18-LC	33.2	31.1	34.9	16.8
(8) 0.8L25-H0.18V0.18-LC	34.8	31.2	41.9	20.0
(9) 0.7H19-H0.08V0.64-LC	30.3	26.0	49.4	18.7
(10) 0.7H19-H0.18V0.64-LC	30.6	26.0	48.4	18.0
(11) 0.7H19-H0V0.64-LC	28.5	26.0	42.4	18.7
(12) 0.7H19-H0V0.64-HC	28.1	26.0	45.7	19.9

Table 3 Mechanical properties of reinforcing bars

Specimen	Bar size	Yield strength (MPa)	Tensile strength (MPa)	Elongation (%)
(1) 1.5L22-H0V0.36-0	D6	467	541	10
(2) 1.5H22-H0V0.36-0	D10	355	504	26
(3) 0.8L22-H0V0.36-0	D13	335	473	27
(4) 0.8H22-H0V0.36-0	D22	333	498	22
(5) 0.8L10-H0.18V0.18-LC	D6	328	499	24
(6) 0.8L16-H0.18V0.18-LC	D10	357	502	25
(7) 0.8L25-H0.18V0.18-LC	D16	347	514	25
	D25	364	531	30
(8) 0.8L19-H0.18V0.18-LC	D6	434	-	-
	D10	377	-	-
	D19	354	-	-
(9) 0.7H19-H0.08V0.64-LC	D6	386	505	24
(10) 0.7H19-H0.18V0.64-LC	D10	357	501	25
(11) 0.7H19-H0V0.64-LC	D13	352	497	27
(12) 0.7H19-H0V0.64-HC	D19	334	489	25



(a) Under long term axial loading



(b) Under mechanism condition

Fig. 3 Relationship between axial compression and horizontal length of masonry walls

VERTICAL AXIAL LOAD

Fig. 3 (a) is the plot showing the relationship between the vertical axial stress obtained from the analysis and the length of first-story walls of five-story masonry buildings, AIJ [1]. The axial compression stress (σ_n) is obtained by dividing the long-term vertical axial load (N), which is supported by the first-story masonry walls in some typical five-story medium-rise residential buildings in Japan by the product of the length of wall (l_0) and the thickness of wall (t_w). It can be seen that the length of wall does not have much effect on the value of axial compression, which is more or less defined. However, the average value of axial compressive stress for the entire wall is 0.81MPa. On the other hand, the plot shown in Fig. 2.2 (b) is the relationship between the wall length and the axial stress ($l\sigma_n + E\sigma_{mu}$) obtained from the analysis based on the beam failure mechanism of the whole building. Here, (σ_{mu}) is the axial stress of the first-story wall corresponding to the total shear force acting at the respective floor beams during mechanism. In this plot, the values of axial compressive stress under mechanism condition vary depending upon the shape of beams and reinforcement, from about -1.4 to +3.4MPa. In the present study, the axial stress of 0MPa is considered when the axial load is not applied, 0.84MPa is chosen as being the average vertical axial stress on the first-story walls of a five-story

building and the axial stress of 1.80MPa is considered as the high axial compression. Further, these three levels of vertical axial loadings have been considered to investigate their effects on the behavior of masonry walls.

INFLECTION POINT

Figure 4 shows the plot between the **inflection height ratio** (y) i.e. the ratio of height of inflection point (h') to the wall height (as defined in this paper), and horizontal length of first floor walls of five-story masonry buildings, AIJ [1]. This ratio indicates the values corresponding to the flexural deformation of the walls under the action of lateral loads (taking standard shear coefficient $C=0.2$) and for those walls in the first floor of the five-story building whose horizontal length in any particular direction is less than 5.5m. The solid circles in the plot indicates the inflection height ratio obtained for a building, assuming that the whole building having rigid floor diaphragms to act as one unit (or plane) of structure, and neglecting the torsional effect. The open circles represent the value obtained by assuming that each frame located in each wall line of building will behave independently. The open triangles represent those values of inflection height ratio of the first-story walls of the other five-story building having plane wall arrangement and are obtained by assuming that each wall line of building will behave independently. What could be understood from the figure is that the values for inflection height ratio (y) of the first-story walls in five-story building due to the flexural deformation under the action of lateral forces lie within a range of about 0.6 to 1.4, and the average value for all the walls is about 0.88 (represented by dashed-and-dotted line in the plot). In the present experimental study, inflection height ratios of 0.67, 1.08 and 1.11 (represented by solid horizontal lines) are considered as shown in Table 1 against the respective specimens. Using these values, the heights of point of application of lateral loads (h') become equal to 0.67, 1.08 and 1.11 times the wall height (h_0).

TEST SETUP AND TEST PROCEDURE

The test setup adopted in the present study is illustrated in Fig.5. Test setup consisted of steel reaction frames and two hydraulic actuators, fixed to the frame in order to simulate the constant vertical loads and in plane lateral repeated forces. The constant vertical loads of 0.84MPa and 1.80MPa were applied to the specimens by a main hydraulic jack with 2,000kN capacity. The repeated lateral forces were applied to the specimen by a double-

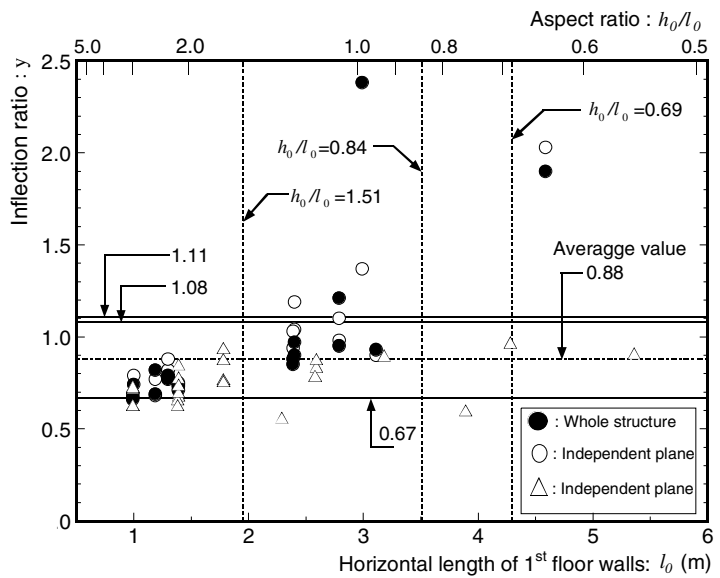


Fig. 4 Relationship between inflection height ratio and horizontal length of masonry walls

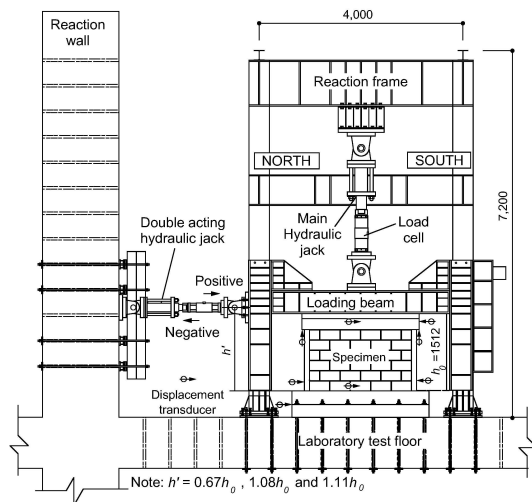


Fig. 5 Test setup

acting hydraulic jack with 1,000kN capacity, placed laterally and fixed to the testing frame and reaction wall. The heights (h') of the longitudinal axis of the lateral forces applied to the specimens (or height of the inflection point) are $0.67h_0$, $1.08h_0$ and $1.11h_0$, where h_0 is the height of wall measured from the top of the footing beam. The measuring instruments such as displacement transducers and strain gauges were installed at desired locations to measure displacements and stains in steel Re-bars and wall.

Each test was first conducted under lateral load control, and then changed to the lateral displacement control as the specimen became more flexible during testing. The data were recorded at certain intervals and also the cracks were marked as they occurred. The load and all the instrument measurements were continuously and automatically scanned and recorded on hard disk and then analyzed in personal computer.

TEST RESULTS

Crack patterns

Final crack patterns of selected specimens are shown in Fig. 6. For the specimens (1) 1.5L22-H0V0.36-0 and (2) 1.5H22-H0V0.36-0 in Fig. 6 (a) with aspect ratio, (h_0/l_0) of 1.51, cracks were concentrated along the diagonals. However, the cracks in specimen (1), which failed in shear, were observed to be converging towards the center extending through the blocks whereas in case of the specimen (2), which failed in flexural failure mode, the cracks were observed mostly along the horizontal joint mortar. Depending upon the modes of failure, similar crack patterns were developed in the specimens (5) and (6) in Fig. 6 (b) with aspect ratio (h_0/l_0) 0.84, which failed in flexure and shear failure modes respectively. The specimens (9) and (10) in Fig. 6 (c) both failed in shear and thus showed a much more uniform inclined cracking. At failure, the cracks penetrated into the confining columns showing a rapid reduction in the lateral load carrying capacity of the specimens.

Hysteresis curves

The hysteresis loops of the applied lateral load (Q) versus story drift (R) response curves for the selected models are shown in Figs.7 and 8. The

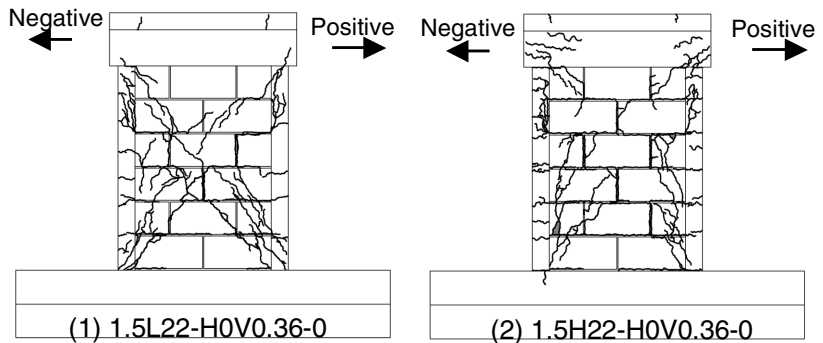


Fig. 6 (a) Specimens with aspect ratio (h_0/l_0) of 1.51

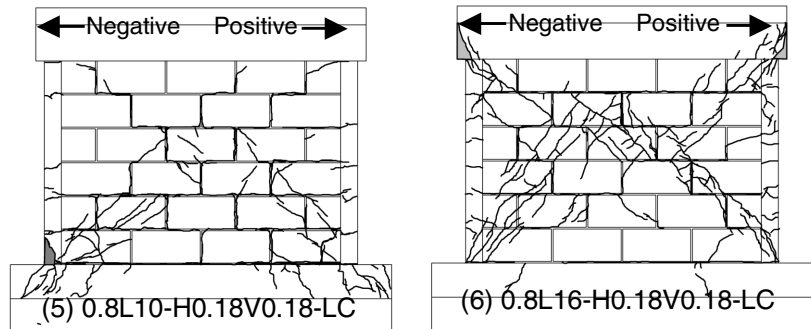


Fig. 6 (b) Specimens with aspect ratio (h_0/l_0) of 0.84

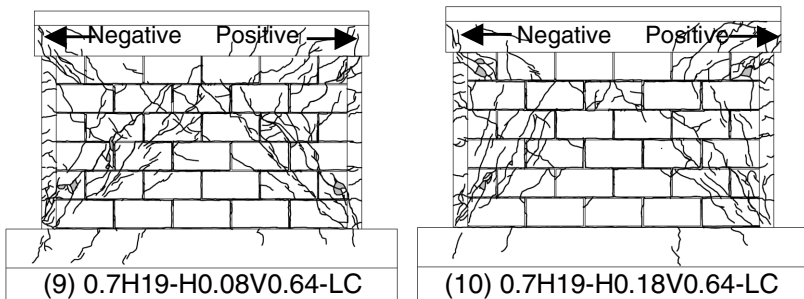


Fig. 6 (c) Specimens with aspect ratio (h_0/l_0) of 0.69

figures are drawn to the same scale to allow for the comparison among the Q-R relations of the specimens. The story drift (R) is defined as a story displacement between top and bottom of the wall divided by the wall height (h_0) of the specimen measured from top of the foundation beam, and the mean shearing stress ($\bar{\tau}$), which is obtained by dividing the applied lateral load by the gross horizontal cross-sectional area of the wall, are also shown in these figures. The dotted lines in the figures represent the theoretical values determined by the ultimate flexural moment capacity at the bottom of each wall (V_{mu}), while the dashed lines represent the ultimate lateral strengths determined in shear failure mode of the wall with flexural reinforcement in its wall edges or R/C confining columns (V_{su}). The three types of failure modes observed are shown as S for shear, SL for sliding and F for flexure inside these figures.

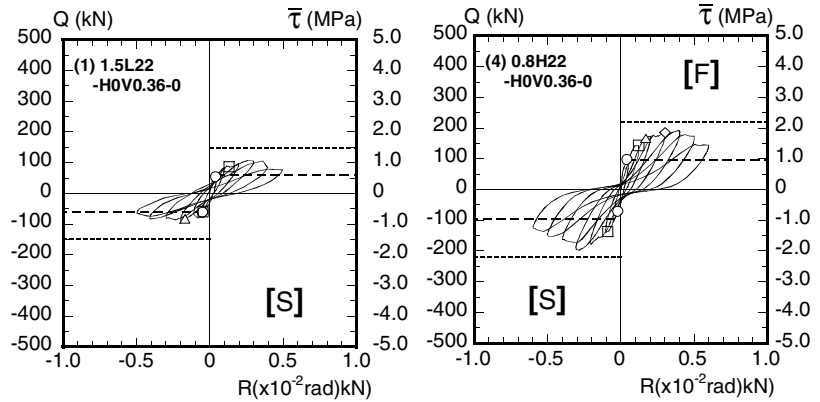


Fig. 7 Q-R hysteresis loops of H0V0.36-0 series

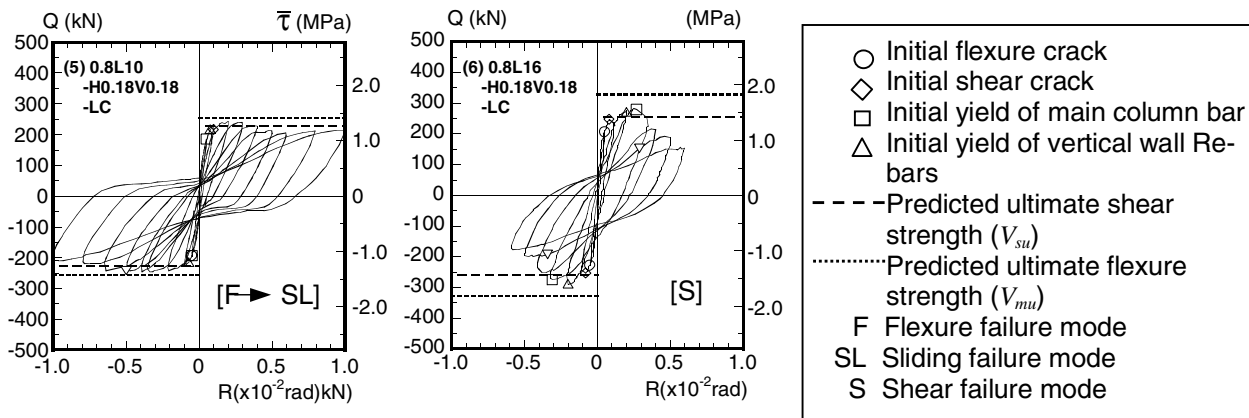


Fig. 8 Q-R hysteresis loops of H0.18V0.18-LC series

Notations used in Figs. 7 and 8

Load-displacement envelope curves

Envelope curves of lateral load in terms of shearing stress, ($\bar{\tau}$) versus story-drift relations obtained from the Q-R hysteresis loops of all the specimens are presented in Figs. 9 (a) through (c), where the lateral forces (Q) are given by the simple average calculated from the North- and South-side, that is, positive and negative loading curves. In all curves shown, the plotted drift is on the basis of horizontal top displacement without any correction for slip (for the specimen which exhibited a sliding failure). The failure modes are also indicated by different symbols as shown in the figures. The shape of the envelope curves beyond the maximum ultimate load varies from one wall specimen to another specimen depending upon the level of axial stress, percentage of wall reinforcement, point of inflection, etc.

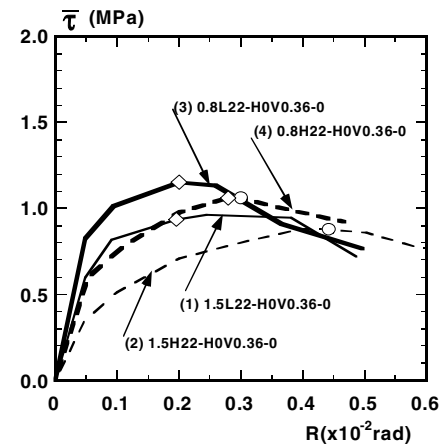


Fig. 9 (a) $\bar{\tau}$ - R envelope curves for same tension reinforcement ratio

In addition, theoretical ultimate strengths for all the twelve specimens are also shown in Table 4 together with the expected failure modes and observed test results.

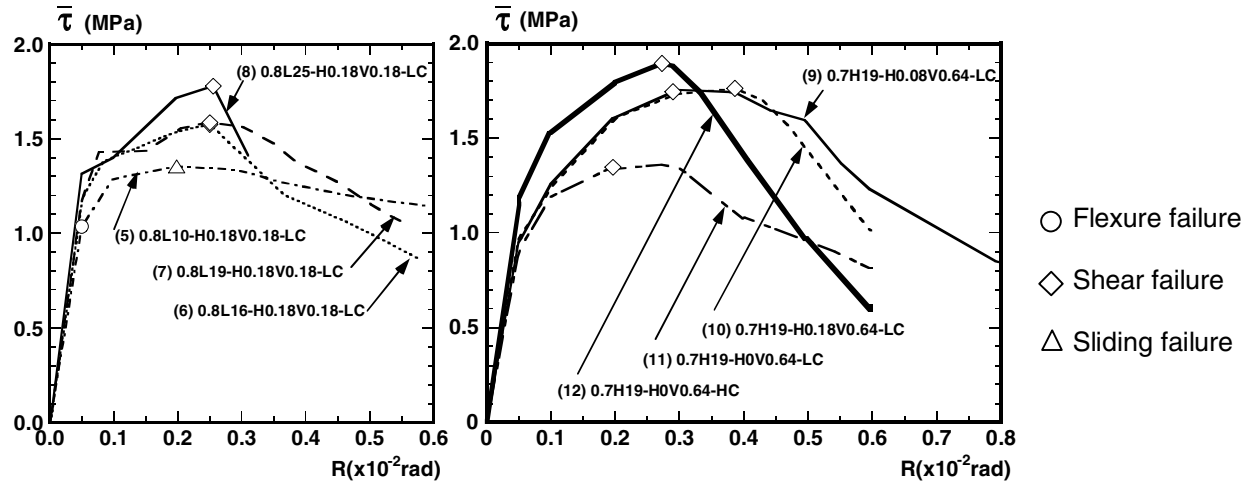


Fig. 9 (b) $\bar{\tau}$ - R envelope curves for different tension reinforcement ratio

Fig. 9 (c) $\bar{\tau}$ - R envelope curves for different constant vertical axial loads

Table 4 Predicted and observed ultimate lateral strengths and failure modes

Specimen	Experimental value				Theoretical value			Ratio of experimental and theoretical values			
	Ultimate strength		Observed Failure mode		Ultimate flexural strength V_{mu} (kN)	Ultimate shear strength V_{su} (kN)	Predicted Failure mode	$\frac{Q_{max}}{V_{mu}}$		$\frac{Q_{max}}{V_{su}}$	
	Q_{max} (kN)	$\left(\bar{\tau}_{max} = \frac{Q_{max}}{A_v} \right)$ (MPa)						①	②	①	②
	Positive	Negative	Positive	Negative	③	④	③	③	④	④	
①	②										
(1) 1.5L22-H0V0.36-0	107 (1.07)	89 (0.89)	S		148	59 (0.59)	S	0.72	0.60	1.82	1.51
(2) 1.5H22-H0V0.36-0	94 (0.94)	88 (0.88)	F		89	40 (0.40)	S	1.06	0.99	2.33	2.18
(3) 0.8L22-H0V0.36-0	207 (1.15)	208 (1.16)	S		364	126 (0.70)	S	0.57	0.57	1.64	1.65
(4) 0.8H22-H0V0.36-0	192 (1.07)	196 (1.09)	F	S	220	96 (0.53)	S	0.87	0.89	2.00	2.04
(5) 0.8L10-H0.18V0.18-LC	244 (1.36)	246 (1.37)	F→SL		254	228 (1.27)	F	0.96	0.97	1.07	1.08
(6) 0.8L16-H0.18V0.18-LC	283 (1.57)	290 (1.61)	S		328	257 (1.43)	S	0.86	0.88	1.10	1.13
(7) 0.8L19-H0.18V0.18-LC	300 (1.67)	285 (1.58)	S		387	261 (1.45)	S	0.78	0.74	1.15	1.09
(8) 0.8L25-H0.18V0.18-LC	320 (1.78)	310 (1.72)	S		522	298 (1.65)	S	0.61	0.59	1.08	1.04
(9) 0.7H19-H0.08V0.64-LC	380 (1.73)	391 (1.78)	S		501	278 (1.26)	S	0.76	0.78	1.37	1.41
(10) 0.7H19-H0.18V0.64-LC	396 (1.80)	379 (1.72)	S		501	295 (1.34)	S	0.79	0.76	1.34	1.28
(11) 0.7H19-H0V0.64-LC	297 (1.35)	307 (1.40)	S		501	229 (1.04)	S	0.59	0.61	1.30	1.34
(12) 0.7H19-H0V0.64-HC	405 (1.84)	418 (1.90)	S		637	361 (1.64)	S	0.64	0.66	1.12	1.16

DISCUSSIONS

Factors affecting ultimate lateral strengths

Some of the factors affecting the ultimate lateral load carrying capacity of the specimens are discussed.

Effect of shear span ratio

The shear span ratio is related to the aspect ratio (i.e. height to length ratio) and the inflection height ratio. Herein, $\bar{\tau}$ - R envelope curves of the test specimens (1)~(4) with different shear span ratios are compared

each other and as shown in Fig. 9 (a), the ultimate lateral load carried by the specimens with low inflection point (i.e. specimens (1) and (3) represented by solid lines) is seen to be higher than the specimens with high inflection point (i.e. specimens (2) and (4) shown by dashed lines). In other words, the lateral strengths of the specimens increase with the decrease of shear span ratio. Likewise, it can be seen that the specimens (2) and (4) having higher inflection point ratio underwent flexural failure as shown by dashed lines. However, for the same height of point of inflection, it can be seen that the lateral load carrying capacity of the specimens (3) and (4) with low aspect ratio shown by solid lines is higher than the specimens (1) and (2) with high aspect ratio.

Effect of tensile reinforcement ratio

From the $\bar{\tau}$ -R envelope curves of the specimens (5)~(8) shown in Fig. 9 (b), the ultimate lateral strength increases with the increase of the amount of steel reinforcement in the confining R/C columns and after developing the maximum value, the strength deteriorates with the increase in lateral displacement. However, there is not much difference in maximum lateral strengths of the specimens (6) and (7). This might be possible due to the reasons; firstly the difference in their tension reinforcement ratio (0.11 and 0.16 as shown in Table 1) is comparatively small and both failed in shear failure mode, and secondly the difference in their theoretical ultimate shear strengths ($261/257=1.02$ as shown in Table 3) is also very small.

Effect of vertical axial stress

Since there is only one specimen (12) tested under high axial compression, it would be appropriate to compare the $\bar{\tau}$ -R envelope curves of specimens (9)~(12) shown in Fig. 9 (c). As indicated by the curves, it is evident that the increase in vertical axial stress tends to increase the ultimate lateral strength of the specimens. Its effect is substantial when comparing the envelope curve of specimen (12) with that of specimen (11) while it is not significant when compared to the curves of (9) and (10).

Prediction of ultimate strengths using existing equations

The predicted theoretical values, given in Table 3, for ultimate flexural strength (V_{mu}) and ultimate shear strength (V_{su}) for all the masonry wall specimens were determined by the existing equations discussed below.

Ultimate strengths

The ultimate shear strengths of the confined concrete hollow block masonry specimens (V_{mu}) corresponding to the ultimate flexural moment were calculated from the following equation recommended by AIJ Standards [2].

$$V_{mu} = (a_l \cdot \sigma_y \cdot l_w + 0.5a_w \cdot \sigma_{wy} \cdot l_w + 0.5N \cdot l_w) / h' \quad (1)$$

where V_{mu} : ultimate lateral shear strength corresponding to the ultimate flexural moment (N), a_l : cross-sectional area of longitudinal Re-bar in confining column (mm^2), σ_y : yield strength of longitudinal Re-bar in confining column (MPa), l_w : center to center distance between of longitudinal Re-bar in two confining columns (mm), a_w : cross-sectional area of vertical wall reinforcing bars (mm^2), σ_{wy} : yield strength of vertical wall reinforcing bars (MPa), N : vertical axial load acting on the masonry wall (N), and h' : height of inflection point (mm).

The ultimate shear strengths of confined reinforced concrete hollow block masonry wall specimens (V_{su}) were calculated from the following equation recommended by Matsumura [3].

$$V_{su} = \left\{ k_u \cdot k_p \left[\frac{0.76}{\left(\frac{h}{d} + 0.7 \right)} + 0.012 \right] \sqrt{F_m + 0.18\gamma \cdot \delta \sqrt{p_h \cdot h \cdot \sigma_y \cdot F_m} + 0.2\sigma_0} \right\} \cdot t \cdot j \cdot 10^3 \quad (2)$$

where V_{su} : ultimate lateral shear strength (kN), k_u : reduction factor equal to 0.64, k_p : $1.16p_t^{0.3}$ ($p_t = a_t/(t \cdot d)$ in %), h : height of the masonry wall (m) and in this paper it is taken as equal to $2h'$ (h' is the height of inflection point), d : distance between the compression extreme fiber in masonry wall and the tension bar in the confining columns ($=l_0-t/2$) (m), F_m : compressive strength of prism (MPa), γ : strength reduction factor due to the presence of mortar joints, and is equal to 0.6 for the present case, δ : factor concerning loading method equal to 1.0, p_h : horizontal steel reinforcement ratio, $h\sigma_y$: yield strength of horizontal reinforcing steel bar (MPa), σ_0 : vertical axial stress (MPa), t : thickness of the masonry wall (m), l_0 : length of wall (m), and j : distance between the forces of compression and tension assumed as $7/8d$ (m).

Theoretical versus observed ultimate strengths

The observed maximum ultimate strengths (Q_{max}) of the test specimens were compared to their predicted theoretical values V_{su} and V_{mu} obtained from the above Equations (1) and (2) to investigate the variation between these values. The ratio of experimental to theoretical values, that is, Q_{max}/V_{su} and Q_{max}/V_{mu} of all the specimens, both under positive and negative loadings, are presented in Table 3. For three specimens (2), (4) and (5) that failed in flexural failure mode, the observed flexural strengths are about 0.87~1.06 times V_{mu} , which was calculated from Equation (2). This implies that the theoretical value for ultimate flexural strength can be well predicted by the existing equation. On the other hand, the Q_{max}/V_{su} values of almost all the specimens which failed in shear failure mode vary from 1.04 to 2.04 indicating that the theoretical values are slightly being overestimated by Equation (2). Therefore, it might be necessary to examine the validity of the items or correctness of coefficients in the equation.

Examining for possible correction to ultimate shear strength equation

As mentioned above, an attempt is made to discuss and find out the items or coefficients in the equation causing the inaccurate estimation of ultimate shear strengths, which were generally found to be lower than the actual experimental values.

Effect of axial stress (σ_0) on ultimate shear stress (τ_u)

Fig. 10 shows the relationship between the ultimate shear stress (τ_u) and the vertical axial stress (σ_0) of the test specimens. With the exclusion of two specimens, that are, (11) 0.7H19-H0V0.64-LC and (12) 0.7H19-H0V0.64-HC, all the remaining specimens shown in the figure were tested in the present structural engineering laboratory in the past years, Yoshimura [4]. Herein, the ultimate shear stress (τ_u) was obtained by dividing the maximum lateral load ($\pm Q_{max}$) by $t \cdot j$, which is the quantity in ultimate shear strength equation. The solid circles represent the values of the present specimens (11) and (12) separately for positive and negative loadings, while the remaining symbols represent the previous test results. The lines in the figure represent the linear regression lines obtained by method of least squares. Based on the past test results, the coefficient contributed by the axial load in the third term of the above equation (2) have been worked out to be 0.71, that is simple average between

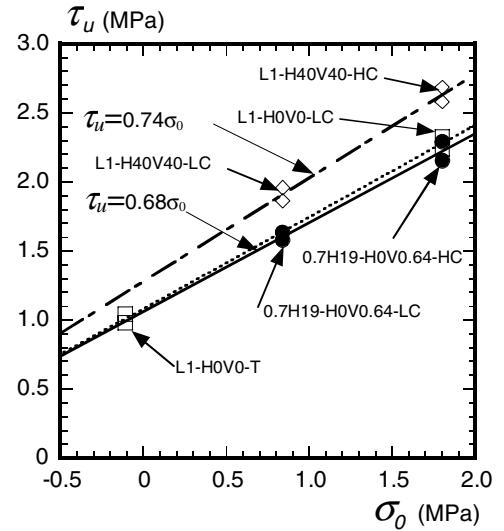


Fig. 10 Ultimate shear stress (τ_u) and vertical axial stress (σ_0)

0.74 and 0.68. Now, considering only the test results of the present study it is seen that these values fall closer to the regression line represented by the full line and the value of the coefficient, which is given by the slope of the line is approximately 0.64 and is slightly smaller as compared to 0.71. Further, it is to be noted that the height of inflection point adopted in the past study was $0.67h_0$ while in the present study the inflection height considered was $1.08h_0$. Although the test results did not yield the same coefficient value, it can be concluded that the vertical axial stress has an effect on the ultimate shear stress irrespective of whether the height of inflection is low or high. Hereafter, for further discussion, the coefficient 0.71 obtained from the past test results will be adopted in the third term of the equation, that is, $0.71\sigma_0$.

Effect of horizontal wall reinforcement ($p_h \cdot h \sigma_y$) on ultimate shear stress (τ_u)

The second term of the ultimate shear strength equation (2), includes the effect of horizontal wall reinforcement. In order to investigate this, four specimens, namely, (9) 0.7H19-H0.08V0.64-LC, (10) 0.7H19-H0.18V0.64-LC, (11) 0.7H19-H0V0.64-LC and (12) 0.7H19-H0V0.64-HC were tested under high inflection point of $1.08h_0$. The results are shown in Fig. 11 representing $\tau_{u(\sigma_0=0)}$ and $\sqrt{p_h \cdot h \cdot \sigma_y \cdot F_m}$ relations, where the vertical

axis is the ultimate shear stress at $\sigma_0=0$, that is, obtained by subtracting the vertical axial stress component equal to $0.71\sigma_0$ from the ultimate shear stress (τ_u) at ultimate lateral loads using equation (2) or is given by ($\tau_{u(\sigma_0=0)} = \tau_u - 0.71\sigma_0$). And the horizontal axis is given by $\sqrt{p_h \cdot h \cdot \sigma_y \cdot F_m}$. The symbols in the plot show the test results of respective specimens under positive and negative loadings. The specimens (11) 0.7H19-H0V0.64-LC and (12) 0.7H19-H0V0.64-HC have no horizontal reinforcements ($p_h=0$) and therefore the test results lie on the vertical axis as shown in the figure. Under this condition, the factor 0.108 ($0.18\gamma\delta$ putting $\gamma=0.6$ and $\delta=1.0$) associated with $\sqrt{p_h \cdot h \cdot \sigma_y \cdot F_m}$ is obtained as represented by the slope of the dotted line. The test results of other two specimens, (9) 0.7H19-H0.08V0.64-LC and (10) 0.7H19-H0.18V0.64-LC with horizontal reinforcements are seen to be well above the dotted line, indicating their effect on the ultimate shear stress of wall specimen.

Effect of aspect ratio (h/d) on ultimate shear stress (τ_u)

One of the parameters within the first term of the existing equation (2) affecting shear stress is the aspect ratio (h/d), which are shown on the horizontal axis of the plot in Fig. 12. And (τ_u) obtained from the equation (3) is plotted on the vertical axis. The ultimate shear stress at the maximum ultimate lateral strength (Q_{max}) obtained from the relation, $_{test}\tau_u = Q_{max} / (t \cdot j)$ and putting this into equation (2) and rearranging the terms suitably, we get the equation (3) as below:

$$\tau'_u = \frac{_{test}\tau_u - 0.18\gamma\delta\sqrt{p_h \cdot h \cdot \sigma_y \cdot F_m} - 0.71\sigma_0}{k_u \cdot k_p \cdot \sqrt{F_m}} \quad (3)$$

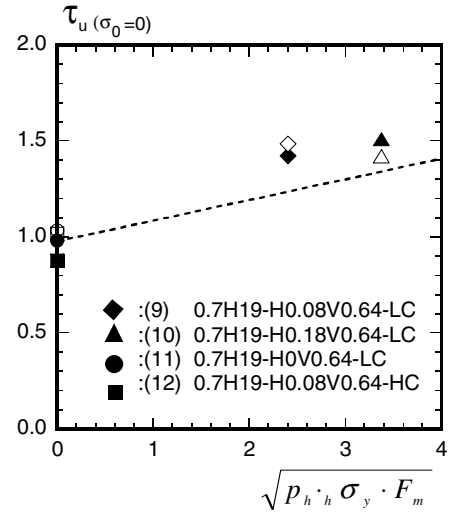


Fig. 11 $\tau_{u(\sigma_0=0)}$ and $\sqrt{p_h \cdot h \cdot \sigma_y \cdot F_m}$ relations

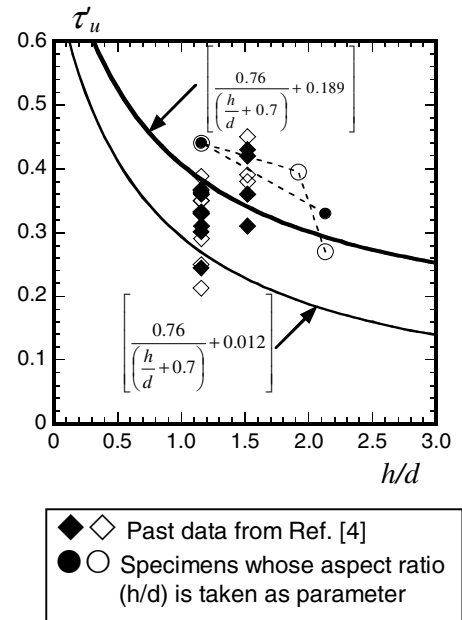


Fig. 12 Aspect ratio (h/d) and shear stress (τ_u) relationship

The experimental data are shown in the figure both for positive and negative loadings, which are represented by the symbols, \blacklozenge , \bullet and \diamond , \circ , respectively. And the dashed lines joining the points, \bullet , and \circ , represent the test specimens with arrangement of horizontal wall reinforcement for which the aspect ratio (h/d) is taken as the parameter. Further, amongst the results other specimens represented by the symbols, \blacklozenge and \diamond , include the past test data, Yoshimura [4] of the past six specimens that failed in shear. As can be seen from the figure, the light solid curve representing the part of first term of the existing equation (2) shows that its value is comparatively lower than the experimental values. Therefore, the factor 0.012 in this term is corrected to 0.189 shown by the heavy solid curve that best fits within the test data.

Accuracy of ultimate shear equation

The relation between the experimental and calculated ultimate shear strengths is shown in Fig. 13. In Fig. 13 (a), the predicted values are the values calculated from the equation (2) without any correction and those values in Fig. 13 (b) are the predicted values from the equation (4) which have been revised by replacing the factor 0.012 by 0.189 and $0.2\sigma_0$ by $0.71\sigma_0$. From Fig. 3 (a) it can be seen that the experimental values are generally higher than the predicted strength values. However, the theoretical values predicted by the corrected equation become almost closer to the experimental ultimate strengths.

$$V_{su} = \left\{ k_u \cdot k_p \left[\frac{0.76}{\left(\frac{h}{d} + 0.7\right)} + 0.189 \right] \sqrt{F_m + 0.18\gamma \cdot \delta \sqrt{p_h \cdot h \cdot \sigma_y \cdot F_m + 0.71\sigma_0}} \right\} \cdot t \cdot j \cdot 10^3 \quad (4)$$

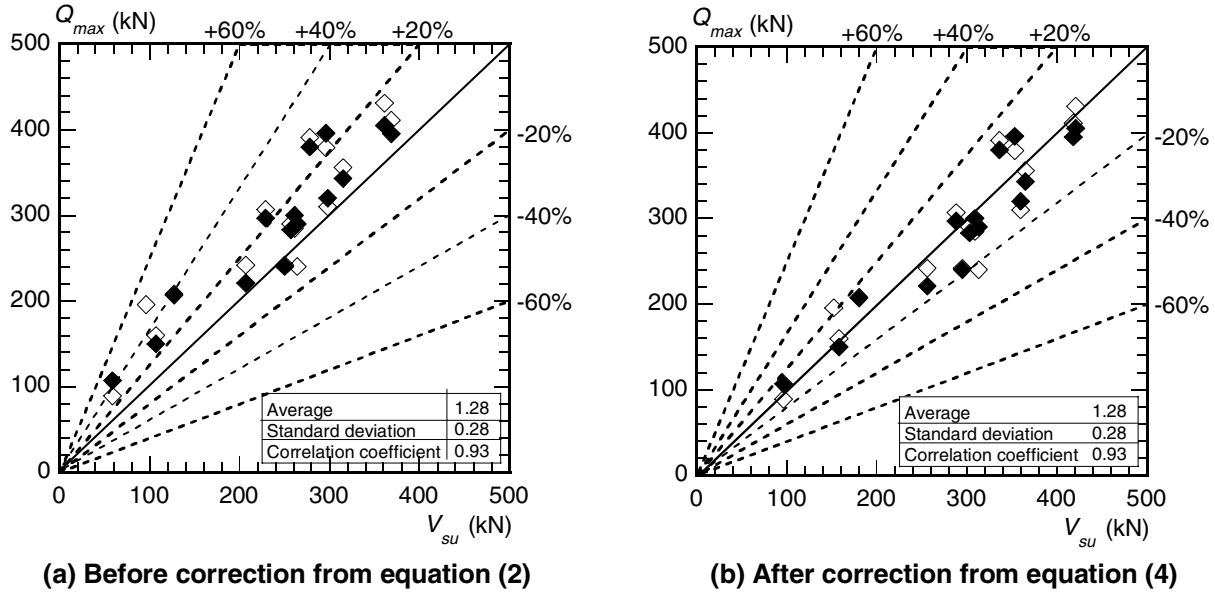


Fig. 13 Relationship between experimental (Q_{max}) and predicted (V_{su}) ultimate strengths

CONCLUSIONS

The experimental study was conducted to investigate the seismic performance of the confined concrete hollow block masonry walls considering the parameters such as height of inflection point ($0.67h_0$, $1.08h_0$ and $1.11h_0$), shear span ratio ($M/Qd = 0.58 \sim 1.77$) for aspect ratios (1.51, 0.84 and 0.67), tensile reinforcement ratio ($p_t = 0.04 \sim 0.29\%$), horizontal wall reinforcement ratios ($p_h = 0\%$, 0.08% and 0.18%) and vertical axial stress ($\sigma_0 = 0.84$ and 1.8MPa). The present test results were also compared with the test

results of past in order to investigate the accuracy of the terms or factors in the existing equation. Based on the observations during tests and analysis of data, the following conclusions were obtained.

Irrespective of the height of point of application of lateral forces to the specimens, that is, whether the inflection point is low or high, it may be concluded that the vertical axial load has positive effect on the value of ultimate shear stress of the specimens.

The effect of different amount of horizontal wall reinforcement on the ultimate shear stress, which is expressed by second term of the existing equation (2), could not be assessed clearly while it is evident that the wall reinforcements contribute to the ultimate lateral shear strength of the walls.

The factor of 0.012 in the first term of the shear equation (2), is suggested to be replaced by the value of 0.189 obtained from the test results.

ACKNOWLEDGEMENT

The authors deeply express sincere appreciation to Japan Society for Promotion of Science (JSPS) for financial support that made possible to carry out this experimental study. Further, thanks are extended to Mr. T. Hiramatsu, Ms. F. Kankura and all other students of the Structural Engineering Laboratory of Oita University for their assistance during the study.

REFERENCES

1. AIJ Standards for Structural Design of Masonry Structures, 1997, pp.127~133, in Japanese.
2. AIJ, "Ultimate Strength and Deformation Capacity of Buildings in Seismic Design", 1990, pp.592-593, in Japanese
3. Matsumura, A., "Shear Strength of Reinforced Masonry Walls", Proceeding of 9th World Conference on Earthquake Engineering, pp. VI-121-126, Tokyo-Kyoto, 1988.
4. Yoshimura, K., Kikuchi, K., Kuroki, M., Liu, L., Ma, L., "Effect of vertical loads and repeated lateral forces on seismic behavior of confined concrete masonry walls", 8th Canadian Conference on Earthquake Engineering, Vancouver 1999, pp.107-112.